







# Genetic landscape of external auditory canal squamous cell carcinoma

Kuniaki Sato<sup>1,2</sup>  | Noritaka Komune<sup>2</sup>  | Takahiro Hongo<sup>2,3</sup> | Kensuke Koike<sup>2,4</sup> | Atsushi Niida<sup>5</sup>  | Ryutaro Uchi<sup>2</sup> | Teppei Noda<sup>2</sup> | Ryunosuke Kogo<sup>2</sup> | Nozomu Matsumoto<sup>2</sup>  | Hidetaka Yamamoto<sup>3</sup> | Muneyuki Masuda<sup>1</sup>  | Yoshinao Oda<sup>3</sup>  | Koshi Mimori<sup>4</sup>  | Takashi Nakagawa<sup>2</sup>

<sup>1</sup>Department of Head and Neck Surgery, National Hospital Organization Kyushu Cancer Center, Fukuoka, Japan

<sup>2</sup>Department of Otorhinolaryngology, Graduate School of Medical Sciences, Kyushu University, Fukuoka, Japan

<sup>3</sup>Department of Anatomic Pathology, Graduate School of Medical Sciences, Kyushu University, Fukuoka, Japan

<sup>4</sup>Department of Surgery, Kyushu University Beppu Hospital, Beppu, Oita, Japan

<sup>5</sup>Laboratory of Molecular Medicine, Human Genome Center, The Institute of Medical Science, The University of Tokyo, Tokyo, Japan

## Correspondence

Noritaka Komune, Department of Otorhinolaryngology, Graduate School of Medical Sciences, Kyushu University, 3-1-1 Higashi-ku, Fukuoka, Fukuoka, 860-8556, Japan.

Email: komune.noritaka.233@m.kyushu-u.ac.jp

## Funding information

Japan Society for the Promotion of Science, Grant/Award Number: 18H02951 and 18K16895

## Abstract

External auditory canal squamous cell carcinoma (EACSCC) is an extremely rare and aggressive malignancy. Due to its rarity, the molecular and genetic characteristics of EACSCC have not yet been elucidated. To reveal the genetic alterations of EACSCC, we performed whole exome sequencing (WES) on 11 primary tumors, 1 relapsed tumor and 10 noncancerous tissues from 10 patients with EACSCC, including 1 with a rare case of synchronous bilateral EACSCC of both ears. WES of the primary tumor samples showed that the most frequently mutated gene is *TP53* (63.6%). In addition, recurrent mutations in *CDKN2A*, *NOTCH1*, *NOTCH2*, *FAT1* and *FAT3* were detected in multiple samples. The mutational signature analysis of primary tumors indicated that the mutational processes associated with the activation of apolipoprotein B mRNA-editing enzyme catalytic polypeptide-like (APOBEC) deaminases are the most common in EACSCC, suggesting its similarity to SCC from other primary sites. Analysis of arm-level copy number alterations detected notable amplification of chromosomes 3q, 5p and 8q as well as deletion of 3p across multiple samples. Focal chromosomal aberrations included amplifications of 5p15.33 (*ZDHHC11B*) and 7p14.1 (*TARP*) as well as deletion of 9p21.3 (*CDKN2A/B*). The protein expression levels of *ZDHHC11B* and *TARP* in EACSCC tissues were validated by immunohistochemistry. Moreover, WES of the primary and relapsed tumors from a case of synchronous bilateral EACSCC showed the inpatient genetic heterogeneity of EACSCC. In summary, this study provides the first evidence for genetic alterations of EACSCC. Our findings suggest that EACSCC mostly resembles other SCC.

## KEYWORDS

exome sequencing, external auditory canal cancer, head and neck cancer, squamous cell carcinoma, tumor heterogeneity

This is an open access article under the terms of the Creative Commons Attribution-NonCommercial-NoDerivs License, which permits use and distribution in any medium, provided the original work is properly cited, the use is non-commercial and no modifications or adaptations are made.

© 2020 The Authors. *Cancer Science* published by John Wiley & Sons Australia, Ltd on behalf of Japanese Cancer Association.

## 1 | INTRODUCTION

External auditory canal squamous cell carcinoma (EACSCC) is a rare and aggressive malignant disease originating from squamous epithelial cells of the external auditory canal, which reportedly occurs in 1 to 6 cases out of 1 000 000 individuals per year, with poor overall survival.<sup>1-5</sup> Because of its rarity, an evidence-based treatment strategy for EACSCC has not yet been established; thus, it is clinically and biologically important to elucidate the molecular characteristics of EACSCC to discover novel therapeutic targets.

Recent studies based on next-generation sequencing technologies have identified genetic drivers of rare malignancies, resulting in the discovery of therapeutic vulnerabilities and clinical biomarkers.<sup>6,7</sup> For EACSCC, a previous study using gene expression profiling identified the long noncoding RNA lnc-MMP3-1 as a novel prognostic biomarker.<sup>8</sup> However, the genetic basis of EACSCC and the mechanism that contributes to the development and progression of EACSCC remain poorly understood, in contrast to SCC from other primary sites, such as head and neck SCC (HNSCC)<sup>9</sup> and cutaneous SCC.<sup>10</sup>

Here, we report genetic abnormalities in EACSCC for the first time. Using whole exome sequencing (WES) and bioinformatics analyses, we uncovered the genetic alterations of 10 primary EACSCC cases. Moreover, by analyzing an extremely rare case of synchronous bilateral primary EACSCC (ie, primary EACSCC of both ears) and a locally relapsed tumor, we revealed the inpatient heterogeneity of EACSCC, which is key to understanding its molecular basis

and developing a therapeutic strategy for EACSCC. We also discuss the genetic characteristics of EACSCC by comparing them with those of SCC from other primary sites in this study.

## 2 | MATERIALS AND METHODS

### 2.1 | Ethics statement

The protocol of this study was reviewed and approved by the institutional review boards and ethics committees of Kyushu University (Protocol Number: 700-2 and 30-268). All experiments with human samples were conducted according to the principles expressed in the Declaration of Helsinki.

### 2.2 | Patients and sample collection

Ten patients who provided written informed consent were enrolled in this study. All patients were diagnosed with EACSCC and treated at Kyushu University Hospital Department of Otorhinolaryngology Head and Neck Surgery from September 2015 to March 2019. Tumor clinical stage was defined using the modified Pittsburgh classification.<sup>11</sup> Surgically resected or biopsy samples of EACSCC and matched peripheral blood samples were obtained from the patients. Among 10 patients, patient T939 was diagnosed with synchronous bilateral primary EACSCC of both ears. The primary tumor samples were obtained by tissue biopsy prior to chemoradiotherapy, and recurrent tumor samples in the

**TABLE 1** The clinicopathological characteristics of EACSCC patients

Patient ID	Sex	Age at Dx	Primary site	Clinical stage	Differentiation	Treatment
210T	F	64	L	T2N0M0	Well-Mod	Surgery (LTBR)
111T	F	48	L	T4N0M0	Well	IC (TPF <sup>a</sup> ), Preoperative-CRT (CDDP 100 mg/m <sup>2</sup> x2, RT 66Gy), Surgery (LTBR)
097T	M	66	R	T3N0M0	Well	IC (TPF), CRT (CDDP 100 mg/m <sup>2</sup> x1, RT 66 Gy)
465T	M	79	R	T3N0M0	Well	Surgery (LTBR), Postoperative-CRT (CDDP 80 mg/m <sup>2</sup> x2, RT 60 Gy)
331T	F	78	R	T4N1M0	Well	CRT (CDDP 64 mg/m <sup>2</sup> x2, RT 60 Gy)
704T	M	83	L	T3N0M0	Well	None <sup>b</sup>
328T	F	67	L	T1N0M0	Well-Mod	IC (TPF), Surgery (LTBR)
501T	F	66	R	T3N0M0	Well	IC (TPF), Surgery (LTBR)
981T	F	88	L	T3N0M0	Mod	CRT (CDDP 64 mg/m <sup>2</sup> x2, RT 66 Gy)
939T	F	38	L and R	L: T2N0M0, R: T4N2bM0	Well	i.a. Chemotherapy + RT (DTX 60 mg/m <sup>2</sup> + CDDP 70 mg/m <sup>2</sup> x2, RT 65.4 Gy), Systemic Chemotherapy (FP + Cmab <sup>c</sup> , Weekly PTX 80 mg/m <sup>2</sup> + Cmab 250 mg/m <sup>2</sup> )

Abbreviations: CDDP, cisplatin; CRT, chemoradiation therapy; Cmab, cetuximab; DTX, docetaxel; Dx, diagnosis; EACSCC, external auditory canal squamous cell carcinoma; F, female; i.a., intra-arterial; IC, induction chemotherapy; L, left; LTBR, lateral temporal bone resection; M, male; Mod, moderately differentiated; PTX, paclitaxel; R, right; RT, radiation therapy; Well, well differentiated.

<sup>a</sup>5-FU (600 mg/m<sup>2</sup>, days 1-5) + CDDP (60 mg/m<sup>2</sup>, day 1) + DTX (60 mg/m<sup>2</sup>, day 1), every 3 weeks, one to two cycles.

<sup>b</sup>Best supportive care was selected due to synchronous bile duct cancer.

<sup>c</sup>5-FU (800 mg/m<sup>2</sup>, days 1-4) + CDDP (80 mg/m<sup>2</sup>, day 1) + Cmab (400 mg/m<sup>2</sup> at initial dose, followed by 250 mg/m<sup>2</sup>, day 1, 8 and 15).

right ear were collected. Detailed information on the patients and clinicopathological characteristics are described in Table 1. All collected samples were immediately snap-frozen using liquid nitrogen and stored at  $-80^{\circ}\text{C}$  until DNA extraction. To obtain matched non-cancerous genomic DNA, we collected peripheral blood mononuclear cells (PBMC) from the peripheral blood of the patients.

### 2.3 | DNA extraction, library preparation and whole exome sequencing

The extraction of genomic DNA from the fresh frozen tumor tissues and the patient-matched PBMC was conducted using DNeasy Blood and Tissue Kits (Qiagen, Chatsworth, CA, USA). Library preparation from the extracted DNA and WES were performed at the Beijing Genomics Institute (Shenzhen, China). Library preparation was conducted using an Agilent SureSelect All Exon V6 exome capture kit (Agilent Technologies, Santa Clara, CA, USA). The captured libraries were sequenced using Illumina HiSeq X Ten (Illumina, San Diego, CA, USA) with the paired-end 100-bp sequence read option according to the manufacturer's protocols.

### 2.4 | Alignment and detection of somatic and germline variants

The sequence data were processed through the in-house pipeline Genomon 2.5.2 (<http://genomon.hgc.jp>). Briefly, the sequencing reads were aligned to the NCBI Human Reference Genome Build 37 hg19 with BWA version 0.7.8 using default parameters (<http://bio-bwa.sourceforge.net/>). PCR duplicate reads were removed using Picard (<http://www.picard.sourceforge.net>). Mutation calling was performed using the EBCall algorithm<sup>12</sup> with the following parameters: (a) mapping quality score  $\geq 30$ ; (b) base quality score  $\geq 15$ ; (c) both the tumor and normal depths  $\geq 8$ ; (d) variant reads in tumors  $\geq 4$ ; (e) variant allele frequency (VAF) in the tumor samples  $\geq 0.05$ ; (f) VAF in the normal samples  $< 0.1$ ; (g) minus logarithm of *P*-value of Fisher's exact test  $\geq 1.3$ ; and (h) minus logarithm of the *P*-value of EBCall  $\geq 5$ . In patient T939, germline variants in the DNA derived from PBMC were detected in the same pipeline. Subsequently, the 122 curated pathogenic variants in 48 genes previously reported in a pan-SCC study<sup>13,14</sup> and disease-associated SNP reported in GWAS catalog<sup>15</sup> were screened, followed by manual curation using Integrated Genomic Viewer (IGV).<sup>16</sup>

### 2.5 | Analysis of mutational spectra and signatures

The spectra of single nucleotide variants (SNV) were visualized using the R package MutationalPatterns.<sup>17</sup> For comparison with the mutational signatures in the Catalogues Of Somatic Mutations In Cancer (COSMIC), mutations in the primary tumor samples were allocated to mutational patterns in the COSMIC (Mutational Signatures v3

released in May 2019, <https://cancer.sanger.ac.uk/cosmic/signatures/SBS>) using the same package.

### 2.6 | Estimation of somatic and germline copy number alterations

For estimation of the somatic copy number alterations (CNA) of EACSCC cells, CNVkit version 0.9.0<sup>18</sup> was used on the aligned WES data of the primary and metastatic tumors as well as the PBMC. The somatic CNA were inferred by applying the standard procedure with default parameters (<https://cnvkit.readthedocs.io/en/stable/pipeline.html>). CNA of driver genes in SCC previously reported<sup>19</sup> were examined. The amplified and deleted regions were defined as  $\log_2$ -scaled ratios  $> 0.20$  and  $< -0.20$ , respectively. Subsequently, GISTIC2<sup>20</sup> was used to identify the significantly amplified and deleted chromosomal arms and focal regions across the primary tumor samples using the segmentation data generated by CNVkit. The threshold of the *q*-value was defined as 0.25. In patient T939, the germline CNA of the PBMC sample was estimated using the segment file by "call" command with the "--filter ci" option of the CNVkit.

### 2.7 | Targeted sequencing for validation of somatic mutations

For patient T939 with bilateral EACSCC, the Ion Ampliseq Comprehensive Cancer Panel 2 Kit (Thermo Fisher) was used to validate somatic mutations of *TP53* detected by WES according to the manufacturer's instructions.

### 2.8 | Immunohistochemical analysis

The protein expression levels of *TP53*, *CDKN2A*, *TARP* and *ZDHHC11B* in each EACSCC tissue were evaluated by immunohistochemistry (IHC) as previously described.<sup>21-23</sup> The antibodies used in this analysis were as follows: *TP53* (clone PAB1801, Calbiochem), *CDKN2A* (clone E6H4; CIN Histology Kit, Roche), *TARP* (ab90882, Abcam) and *ZDHHC11B* (HPA057886, Atlas antibodies). The results of IHC were independently reviewed by two pathologists (TH and HY). The IHC status of EACSCC tissues was scored as positive or negative for *TP53* and *CDKN2A*, and as high, low or negative for *TARP* and *ZDHHC11B*. *TP53* was considered positive when more than 10% of the tumor cells had immunoreactive nuclei.<sup>21</sup> *CDKN2A* was considered positive when more than 70% of the tumor cells showed strong and diffuse nuclear and cytoplasmic staining.<sup>24</sup> For *TARP* and *ZDHHC11B*, the positivity was evaluated by the combination of the following two criteria referring to the method previously described.<sup>25</sup> First, the proportion was scored according to the percentage of immunoreactive tumor cells as follows: negative (0%), 0; focal (1%-50%), 1; and

diffuse (>50%), 2. Second, the intensity was scored as negative, 0; weak, 1; and strong, 2. The sum of each score was defined as follows: negative, 0; low, 2; and high, 3-4.

## 2.9 | Analysis of publicly available dataset

The datasets of the somatic mutations for 33 types of malignancies in The Cancer Genome Atlas (TCGA) were downloaded from the MC3 TCGA dataset and analyzed using the R package TCGA mutations.<sup>26</sup> The mutational spectra of nonsynonymous SNV in the primary tumor samples in TCGA data and the primary EACSCC samples were combined into one dataset, followed by hierarchical clustering and estimation of the distribution of the COSMIC signatures in each tumor type. The CNA datasets of SCC in TCGA were obtained from cBioportal (<https://www.cbioportal.org/>).

### 2.10 | Data availability

The WES data have been deposited in the Japanese Genotype-phenotype Archive (<https://www.ddbj.nig.ac.jp/index-e.html>) with the following accession number: JGAS0000000214.

## 3 | RESULTS

### 3.1 | The characteristics of patients with external auditory canal squamous cell carcinoma

A total of 10 Japanese patients with EACSCC were enrolled in this study. The clinical and pathological features of all patients are shown in Table 1. Briefly, 70% of the patients (7/10) were female, the median age at initial diagnosis was 66.5 years (range: 38-88 years) and 80% of the patients (8/10) were initially diagnosed with advanced stage disease (T3 or T4). Among the 10 patients, patient T939 had an extremely rare synchronous bilateral EACSCC of both ears at the initial diagnosis. In addition to obtaining primary tumor tissues from both ears, we obtained relapsed tumor tissue after chemoradiation therapy from this patient. In total, 11 primary tumors, 1 relapsed tumor and 10 patient-matched noncancerous PBMC were subjected to analyses.

### 3.2 | Mutational landscape of primary external auditory canal squamous cell carcinoma

To clarify the genetic alterations of EACSCC, we performed WES on genomic DNA derived from the tumor tissues and the patient-matched PBMC as the controls. The DNA samples were sequenced with a median sequencing depth of 98.16 (range: 84.00-108.3). A median of 84 (range: 27-160) nonsynonymous mutations was detected for each primary tumor sample (Figure 1A) using the

Genomon pipeline. From these data, we estimated that each sample had a median mutation rate of 1.44 (range: 0.46-2.75) mutations per megabase. We detected significantly mutated genes listed in the COSMIC Cancer Gene Census, such as *TP53* (7/11), *CDKN2A* (5/11), *NOTCH1* (5/11), *FAT1* (3/11), *FAT3* (2/11) and *NOTCH2* (2/11), in multiple primary EACSCC samples (Figure 1A). The mutations of these genes were also observed in SCC from other primary sites in TCGA (Figure S1A). Consistent with previous studies,<sup>27,28</sup> IHC for TP53 showed that a positive staining pattern of TP53 and the mutational status of *TP53* are well correlated in EACSCC ( $P = 0.015$ , Fisher's exact test, Figure 1A and Figure S1B). In contrast, *CDKN2A* (p16) was immunohistochemically negative in all of the cases examined (Figure 1A). The profiles of nucleotide substitution of the detected synonymous and nonsynonymous SNV showed that C to T transitions are the most common substitution in these primary tumors (Figure 1B and Figure S1C). The hierarchical clustering of nucleotide substitutions of nonsynonymous mutations showed that EACSCC and SCC from other primary sites in the TCGA dataset belong to the same cluster (Figure S1D). To clarify the mutational patterns of EACSCC, we compared the distributions of the COSMIC single-base-substitution mutational signatures (SBS) of EACSCC and SCC from other primary sites in the TCGA dataset. EACSCC showed a high proportion of signatures associated with endogenous mutational processes, such as SBS2/13 (activation of APOBEC enzyme; 27.59%) and SBS6 (defective DNA mismatch repair; 16.15%), while the smoking-related signature SBS4 was not observed in EACSCC (Figure 1C). Moreover, the hierarchical clustering of EACSCC and 33 types of cancer in TCGA revealed that EACSCC is classified with other SCC, such as HNSCC and cervical SCC, in the same cluster where SBS2/13 are predominant (Figure S2). Together, these data suggest that EACSCC mostly resembles the mutational patterns of SCC from other primary sites.

### 3.3 | Overview of copy number alterations in primary external auditory canal squamous cell carcinoma

Next, we estimated the CNA in these 11 primary EACSCC samples from the WES data using the computational inference algorithms CNVkit<sup>18</sup> and GISTIC2.<sup>20</sup> Gene-level CNA of driver genes in SCC<sup>19</sup> were observed; the cell-cycle regulatory tumor suppressor gene *CDKN2A* was deleted in 36% (4/11) of the samples, whereas oncogenes such as *MYC* (5/11), *PIK3CA* (4/11), *TP63* (5/11) and *SOX2* (5/11) were amplified (Figure 1A). The significantly altered arm-level CNA detected by GISTIC2 were amplifications of 3q, 5p and 8q, as well as deletion of 3p (Figure 2A), which have been reported in a TCGA HNSCC cohort<sup>9</sup> and a pan-SCC study.<sup>29</sup> GISTIC2 analysis identified the significantly amplified and deleted chromosomal loci in the primary tumor samples (Table S1). The notable amplified regions that harbor potential oncogenes included 5p15.33 (*ZDHC11B*, encoding Zinc Finger DHC-Type Containing 11B)

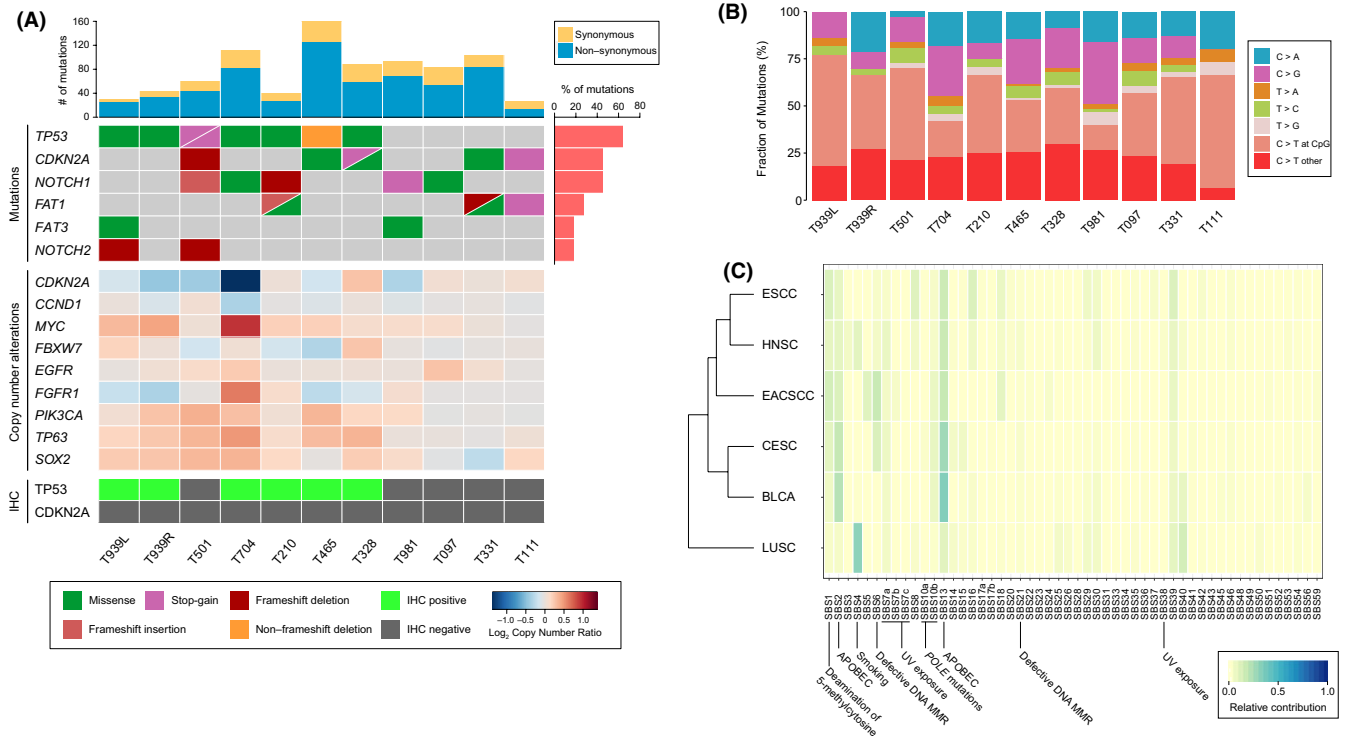


**FIGURE 1** The landscape of genetic alterations in primary external auditory canal squamous cell carcinoma (EACSCC). A, Recurrently mutated genes in primary EACSCC ( $n = 11$ , upper panel). The mutational frequency of each gene per sample (right bars) and the numbers of mutations per sample (upper bars) are shown. The heatmap represents log<sub>2</sub> copy number ratios (red, amplifications; blue, deletions) of the previously reported driver genes in squamous cell carcinoma (middle panel). In the lower panel, the status of immunohistochemistry for TP53 and CDKN2A are shown. See the Materials and Methods section for details about gene selection. B, Stacked bar plots representing the spectra of single nucleotide variants in 11 primary EACSCC samples. C, Heatmap showing the relative contribution of the COSMIC single base substitution (SBS) signatures to the mutational profiles of EACSCC and SCC of different primary sites obtained from TCGA. Signatures with no signals across all cancer types were removed. BLCA, bladder urothelial carcinoma; CESC, cervical squamous cell carcinoma; ESCC, esophageal squamous cell carcinoma; HNSC, head and neck squamous cell carcinoma; LUSC, lung squamous cell carcinoma.

and 7p14.1 (*TARP*, encoding T-cell receptor  $\gamma$  chain alternate reading frame protein) (Figure 2B). The amplification frequencies of *ZDHH11B* and *TARP* in primary EACSCC were 45% (5/11) and 100% (11/11), respectively (Figure 2C). Interestingly, a previous study showed that *ZDHH11B* is overexpressed and acts as an oncogene in lymphoma cells.<sup>30</sup> Likewise, overexpressed *TARP* reportedly promotes tumor growth.<sup>23</sup> In contrast to EACSCC, *ZDHH11B* and *TARP* are not frequently amplified in other types of SCC, suggesting that CNA of these genes might be specific to EACSCC (Figure S3). To examine the expression levels of *ZDHH11B* and *TARP*, we conducted IHC for these proteins. Notably, the cytoplasmic overexpression of *ZDHH11B* in tumor cells was observed in *ZDHH11B*-amplified cases (Figure 2C and D). Moreover, *TARP* protein was immunohistochemically positive in 100% (11/11) of the cases examined (Figure 2C and D). These data suggest that amplifications of these genes could contribute to protein overexpression. Importantly, 9p21.3, which harbors *CDKN2A/B*, was significantly deleted (Figure 2B). The deletion of this locus was observed in primary and metastatic HNSCC,<sup>31</sup> esophageal SCC<sup>32</sup> and cutaneous SCC,<sup>33</sup> suggesting that the loss of function of these genes is a driver event in the carcinogenesis of EACSCC as well as other SCC.

### 3.4 | Inpatient heterogeneity of synchronous bilateral external auditory canal squamous cell carcinoma over space and time

Patient T989 had synchronously occurring bilateral EACSCC of both ears (Figure 3A and B). The primary tumors of the left and right ears were diagnosed as T2N0M0 and T4N2bM0, respectively, and as inoperable. After primary chemoradiation therapy, the tumor of the left ear was diminished, while the tumor of the right ear showed relapse. Although systemic chemotherapies were performed as second-line and third-line treatments, the relapsed tumor progressed and resulted in the death of the patient 15.4 months after the first diagnosis (Figure 3A). We sequenced the pretreatment primary tumor samples and the relapsed tumor samples collected by tissue biopsy. Interestingly, none of the mutations in the primary tumor of the left and right ears overlapped. Although both primary tumors (T939L and T939R) had pathogenic somatic mutations in *TP53*, their genomic positions were different (Figure 3C and Table S2). These results suggest that these tumors were possibly driven independently by different somatic diver mutations. Because recent pan-cancer analysis revealed that pathogenic germline variants are found in multiple types of cancer,<sup>13</sup> we



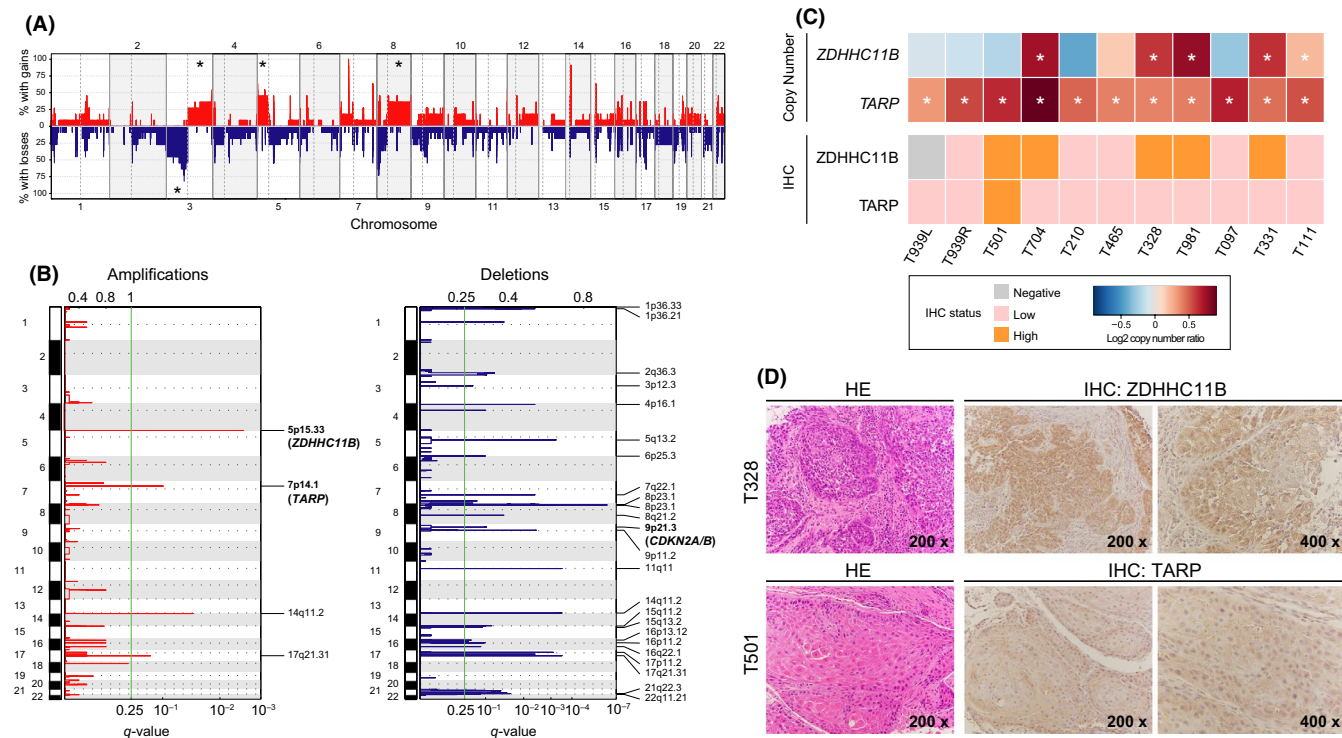


**FIGURE 2** Copy number alterations in primary external auditory canal squamous cell carcinoma (EACSCC). A, Overview of the copy number alterations (CNA) in EACSCC. Bar plots represent the frequencies of the amplifications (red) and deletions (blue) in chromosomal regions across 11 primary EACSCC samples. Asterisks indicate the significantly amplified or deleted chromosomal arms detected by GISTIC2 ( $q$ -value < 0.25). B, Significantly altered chromosomal loci detected by GISTIC2 (left, amplifications; right, deletions). Green lines represent the threshold of significance ( $q$ -value < 0.25). C, The heatmap represents log<sub>2</sub> copy number ratios (red, amplifications; blue, deletions) of ZDHHC11B and TARP (upper panel) in primary EACSCC samples. Asterisks indicate significant amplifications (log<sub>2</sub> copy number ratios > 0.2). Lower panel indicates the status of immunohistochemistry (IHC) for ZDHHC11B and TARP. D, Representative pictures of H&E staining (left panel), IHC for ZDHHC11B (upper right panel) and TARP (lower right panel) of primary EACSCC. The original magnifications are shown in the lower right of each picture.

further examined whether such germline variants or CNA such as deletions of tumor suppressor genes are found in the DNA derived from the PBMC sample of this patient (see Materials and Methods). However, we did not observe any curated pathogenic germline mutations or disease-associated CNA in this sample. Next, we searched for disease-associated single nucleotide polymorphisms (SNP) in the PBMC sample using the online database of genome-wide association studies (GWAS).<sup>15</sup> Interestingly, we found that this patient harbored SNP rs1057941 on 1q22 locus, which is reportedly associated with the risk of multiple cancer types, including lung SCC,<sup>34,35</sup> despite the functional contribution in the onset of EACSCC being unknown (Table S3).

The relapsed tumor sample (T939R-rec) retained 84.8% (28/33) of the mutations observed in the primary tumor sample (T939R). In addition to these “shared” mutations, 23 mutations were observed only in the relapsed tumor sample, while none of these mutations uniquely found in the relapsed tumor sample have been reported as pathogenic mutations or deposited in COSMIC (Figure 3C). The mutation rate of the relapsed tumor sample was increased from 0.57 to 0.85 mutations per megabase, indicating that this relapsed tumor does not show a hypermutation phenotype.<sup>36</sup> In contrast to somatic mutations, we observed that deletion of 2q and amplification of 7p

are predominant in the relapsed tumors compared to the primary tumors (Figure 3D). We did not observe CNA of driver genes in the relapsed tumor compared with the primary tumor (Figure S4). Our data suggest that arm-level CNA may contribute to the recurrence of EACSCC.

## 4 | DISCUSSION

In this study, we determined the genetic landscape of 10 EACSCC cases using WES. The analysis of CNA revealed significantly amplified and deleted chromosomal regions in EACSCC samples that are found in primary and metastatic HNSCC. Moreover, we clarified not only the genetic alterations of the primary EACSCC tumors but also the spatiotemporal changes of the EACSCC genomes in a rare case of bilateral primary and recurrent EACSCC. To our knowledge, this is the first study to examine the genetic alterations of EACSCC.

The analysis of somatic mutations demonstrated that the most commonly altered gene in EACSCC is TP53, which is the most frequently mutated tumor suppressor gene in human cancer, including SCC.<sup>9</sup> We also found that EACSCC harbors recurrent mutations in several genes listed in the COSMIC Cancer Gene Census; mutations

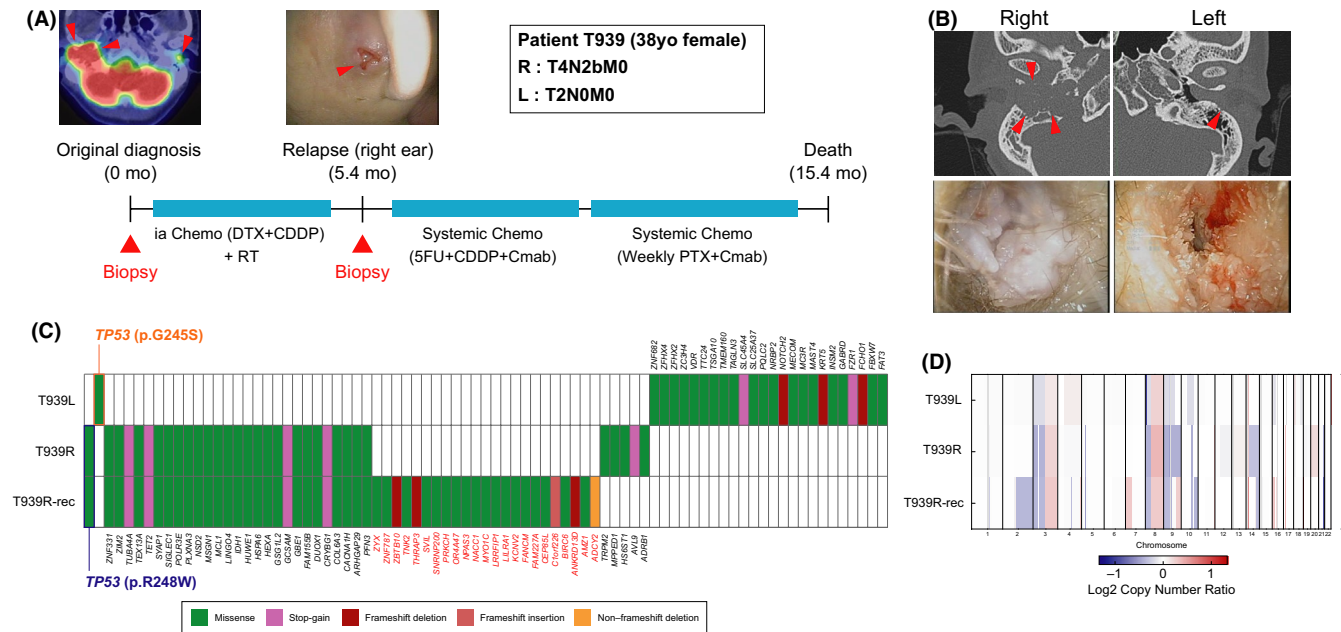


**FIGURE 3** The spatial and temporal intrapatient heterogeneity of bilateral external auditory canal squamous cell carcinoma (EACSCC) in patient T939. A, The clinical time course of patient T939 with bilateral EACSCC. Red arrowheads represent the primary and relapsed tumors. B, Computed tomography (CT) images of patient T939 with bilateral EACSCC. Red arrowheads represent the primary tumors. Otoscopic views of primary tumors are shown in the lower panels. C, The mutational landscape of primary and relapsed tumors in patient T939. The somatic mutations exclusively observed in the recurrent tumor (T939R-rec) are indicated as red-lettered gene symbols. D, Heatmap representing the CNA (red, amplifications; blue, deletions) of the primary and relapsed tumors in patient T939. CDDP, cisplatin; Cmab, cetuximab; DTX, docetaxel; ia Chemo, intra-arterial chemotherapy; PTX, paclitaxel; RT, radiation therapy; Systemic Chemo, systemic chemotherapy; 5FU, 5-fluorouracil.

in *CDKN2A*, *NOTCH1*, *FAT1* and *NOTCH2* are commonly found in multiple types of SCC,<sup>19</sup> suggesting that the major driver mutations of EACSCC are similar to those of other SCC. In addition to these well-characterized somatic mutations, missense mutations in *FAT3* were detected in two primary EACSCC samples and are recurrently found in SCC from other primary sites in TCGA, although the molecular significance of this mutation is still unclear. Moreover, our mutational spectra and COSMIC signature analysis indicated that EACSCC and other SCC in the TCGA dataset belong to the same cluster. These data all suggest that the mutational patterns of EACSCC mostly resemble those of SCC from other primary sites. Unlike lung SCC or HNSCC, tobacco and alcohol use are unlikely to be major carcinogens of EACSCC; previous clinical studies have reported that chronic inflammation in the external auditory canal induced by habitual ear picking and other mechanical stimuli may cause EACSCC,<sup>37,38</sup> but the exact etiology has remained controversial. In this regard, the mutational pattern of EACSCC in which APOBEC signatures are dominant suggests its link to the mutagenic process associated with chronic tissue damage, as a previous genetic study of aggressive cutaneous SCC demonstrated that chronic inflammation-induced APOBEC mutagenesis drives carcinogenesis.<sup>39</sup>

We did not observe overexpression of *CDKN2A* (p16) protein in any primary EACSCC tissues in this study, even in *TP53*-wild-type cases. This result suggests that EACSCC cases in this study are not likely associated with human papilloma virus (HPV) induced-carcinogenesis, which is well characterized in oropharyngeal SCC.<sup>36</sup>

However, because a previous study has demonstrated the presence of HPV DNA in EACSCC tissues,<sup>40</sup> further study is required to clarify the clinical and functional importance of HPV infection in EACSCC.

The CNA in EACSCC also support its genetic similarity to other SCC. A recent pan-SCC study reported that the amplification of chromosome 3q is one of the common CNA in SCC.<sup>29</sup> Importantly, chromosome 3q harbors *ACTL6A* and the master transcription factor *delta-Np63* (N-terminal truncated isoform of *TP63* gene), which repress squamous cell differentiation and activate the YAP1 oncogenic transcription factor in a coordinated manner in HNSCC.<sup>41</sup> Although GISTIC2 analysis did not detect a significant focal gain of these loci, the gain of function of these genes induced by arm-level amplification of chromosome 3q may be an important driving force of carcinogenesis and progression of EACSCC as well as other SCC. Moreover, the focal deletion of the *CDKN2A/B* locus detected in the present study is frequently observed in primary and metastatic solid tumors, including SCC,<sup>42,43</sup> indicating that the deregulated cell cycle control induced by inactivation of these genes might be an important early event in the carcinogenesis of EACSCC. Interestingly, the amplification of 5p15.33 and 7p14.1, which harbor *ZDHH11B* and *TARP*, respectively, were observed in primary EACSCC, although amplification of these loci has not been reported in other SCC. Dzikiewicz-Krawczyk *et al.* (2017) reported that *ZDHH11B* promotes the proliferation of lymphoma cells through a coordinated action with *MYC* and *MYB*.<sup>30</sup> Moreover, *TARP* is overexpressed in several types of cancer and promotes proliferation and invasion of cancer cells.<sup>23,44,45</sup> Importantly,

IHC of the primary EACSCC tissues showed that the overexpression of ZDHHC11B and the copy number amplification are positively correlated, and that TARP is expressed in all of the cases. Thus, their amplification and overexpression might be novel oncogenic mechanisms that promote the development and proliferation of EACSCC. Further investigation is needed to clarify their functional contribution in EACSCC development.

We profiled the genetic aberrations of the primary and relapsed tumors in an extremely rare case with synchronous bilateral EACSCC, patient T939. Our data suggest that two primary EACSCC occurred synchronously through distinct somatic genetic alterations. In addition, we did not observe any pathogenic germline alterations in this patient. In other bilateral malignancies, germline alterations of genes involved in DNA mismatch repair such as *BRCA1/2* in breast cancer<sup>46</sup> and *MSH2/6* in ovarian cancer<sup>47</sup> are reported. Although we did not observe such mutations, it is interesting to note that this patient harbors rs1057941, an SNP associated with risks of multiple cancer types.<sup>34</sup> To elucidate the clinical significance of this SNP, GWAS for EACSCC is warranted.

The relapsed tumor of this patient showed additional somatic mutations and CNA. Although this relapsed tumor was highly resistant to several different chemotherapeutic regimens, the mutation rate of this tumor indicated that it does not show a hypermutation phenotype, suggesting the absence of chemotherapy-induced hypermutation.<sup>36</sup> We did not detect curated driver mutations specific to recurrence; however, it is noteworthy that specific CNA, such as amplification of 7p, became predominant in this relapsed tumor. A computational analysis of pan-cancer genomic data indicated that chromosome 7p harbors potential oncogenes<sup>48</sup>; indeed, several studies have reported that some genes on 7p act as oncogenes through overexpression and gain of function induced by arm-level amplification of the chromosome, with their expression levels positively correlated with aggressive phenotypes.<sup>49,50</sup> Thus, the amplification of 7p may contribute to relapse of EACSCC through these mechanisms.

We acknowledge that there are two limitations in the present study. First, the sample size is limited compared with previously reported large-scale cohorts such as TCGA. Second, integrated analysis in which RNA-seq and ChIP-seq are combined with genomic analysis may provide advantages for a deep understanding of the molecular characteristics and microenvironment of EACSCC; however, we did not conduct such a combined analysis in the current study. Recent studies have shown that dysregulated transcriptional programs not predicted by somatic mutations are powerful driving forces of malignant initiation and progression,<sup>51-53</sup> indicating that these mechanisms may be a key to understanding the aggressiveness of EACSCC and uncovering its therapeutic vulnerabilities. Because previous histopathological studies of EACSCC demonstrated that the presence of laminin5- $\gamma$ 2-stained tumor cells in the primary tumor tissues is positively correlated with poor survival of EACSCC patients,<sup>54,55</sup> transcriptomic dysregulation that induces such alterations might be an important mechanism in the progression of EACSCC. Further study is required to elucidate the bona fide mechanism of carcinogenesis and progression in EACSCC.

In summary, this study provides the first evidence for genetic abnormalities in a rare cohort of EACSCC, as well as the inpatient genetic heterogeneity of EACSCC. Our data could help to understand the molecular pathophysiology of EACSCC and may contribute to the development of therapeutic strategies for the treatment of EACSCC.

## ACKNOWLEDGMENTS

This work used the supercomputing resources provided by the Human Genome Center, Institute of Medical Science, University of Tokyo (<http://sc.hgc.jp/shirokane.html>). We thank Y. Sekino for technical assistance. This work was supported, in part, by the following grants: JSPS KAKENHI 18H02951 and 18K16895.

## DISCLOSURE

The authors have no conflicts of interest to declare.

## ORCID

Kuniaki Sato  <https://orcid.org/0000-0001-6014-1911>

Noritaka Komune  <https://orcid.org/0000-0002-9521-9878>

Atsushi Niida  <https://orcid.org/0000-0002-6851-8004>

Nozomu Matsumoto  <https://orcid.org/0000-0003-0799-6704>

Muneyuki Masuda  <https://orcid.org/0000-0002-7479-8356>

Yoshinao Oda  <https://orcid.org/0000-0001-9636-1182>

Koshi Mimori  <https://orcid.org/0000-0003-3897-9974>

## REFERENCES

1. Prasad SC, D'Orazio F, Medina M, Bacciu A, Sanna M. State of the art in temporal bone malignancies. *Curr Opin Otolaryngol Head Neck Surg.* 2014;22:154-165.
2. Bacciu A, Clemente IA, Piccirillo E, Ferrari S, Sanna M. Guidelines for treating temporal bone carcinoma based on long-term outcomes. *Otol Neurotol.* 2013;34:898-907.
3. Seligman KL, Sun DQ, Ten Eyck PP, Schularick NM, Hansen MR. Temporal bone carcinoma: Treatment patterns and survival. *Laryngoscope.* 2019;130:E11-E20.
4. Allanson BM, Low T-H, Clark JR, Gupta R. Squamous cell carcinoma of the external auditory canal and temporal bone: an update. *Head Neck Pathol.* 2018;12:407-418.
5. Beyea JA, Moberly AC. Squamous cell carcinoma of the temporal bone. *Otolaryngol Clin North Am.* 2015;48:281-292.
6. Sharifnia T, Hong AL, Painter CA, Boehm JS. Emerging opportunities for target discovery in rare cancers. *Cell Chem Biol.* 2017;24:1075-1091.
7. Okuma HS, Kubo T, Ichikawa H, et al. Targeted-sequencing in rare cancers and the impact on patient treatment. *J Clin Oncol.* 2019;37(15\_suppl):e14755-e14755.
8. Liu H, Dai C, Wu Q, Liu H, Li F. Expression profiling of long non-coding RNA identifies lnc-MMP3-1 as a prognostic biomarker in external auditory canal squamous cell carcinoma. *Cancer Med.* 2017;6:2541-2551.
9. Lawrence MS, Sougnez C, Lichtenstein L, et al. Comprehensive genomic characterization of head and neck squamous cell carcinomas. *Nature.* 2015;517:576-582.
10. Pickering CR, Zhou JH, Lee JJ, et al. Mutational landscape of aggressive cutaneous squamous cell carcinoma. *Clin Cancer Res.* 2014;20:6582-6592.
11. Moody SA, Hirsch BE, Myers EN. Squamous cell carcinoma of the external auditory canal: an evaluation of a staging system. *Am J Otol.* 2000;21:582-588.



12. Shiraishi Y, Sato Y, Chiba K, et al. An empirical Bayesian framework for somatic mutation detection from cancer genome sequencing data. *Nucleic Acids Res.* 2013;41:e89.
13. Huang K, Mashl RJ, Wu Y, et al. Pathogenic germline variants in 10,389 adult cancers. *Cell.* 2018;173:355-370.e14.
14. Scott AD, Huang K-L, Weerasinghe A, et al. CharGer: clinical Characterization of Germline variants. Hancock J, editor. *Bioinformatics.* 2019;35:865-867.
15. Buniello A, MacArthur JA L, Cerezo M, et al. The NHGRI-EBI GWAS Catalog of published genome-wide association studies, targeted arrays and summary statistics 2019. *Nucleic Acids Res.* 2019;47:D1005-D1012.
16. Robinson JT, Thorvaldsdóttir H, Winckler W, et al. Integrative genomics viewer. *Nat Biotechnol.* 2011;29:24-26.
17. Blokzijl F, Janssen R, van Boxtel R, Cuppen E. MutationalPatterns: comprehensive genome-wide analysis of mutational processes. *Genome Med.* 2018;10:33.
18. Talevich E, Shain AH, Botton T, Bastian BC. CNVkit: genome-wide copy number detection and visualization from targeted DNA sequencing. *PLOS Comput Biol.* 2016;12:e1004873.
19. Dotto GP, Rustgi AK. Squamous cell cancers: a unified perspective on biology and genetics. *Cancer Cell.* 2016;29:622-637.
20. Mermel CH, Schumacher SE, Hill B, Meyerson ML, Beroukhim R, Getz G. GISTIC2.0 facilitates sensitive and confident localization of the targets of focal somatic copy-number alteration in human cancers. *Genome Biol.* 2011;12:R41.
21. Nakano K, Yamamoto H, Fujiwara M, et al. Clinicopathologic and molecular characteristics of synchronous colorectal carcinoma with mismatch repair deficiency. *Am J Surg Pathol.* 2018;42:172-182.
22. Nakano T, Yamamoto H, Nakashima T, et al. Molecular subclassification determined by human papillomavirus and epidermal growth factor receptor status is associated with the prognosis of oropharyngeal squamous cell carcinoma. *Hum Pathol.* 2016;50:51-61.
23. Yue H, Cai YU, Song Y, et al. Elevated TARP promotes proliferation and metastasis of salivary adenoid cystic carcinoma. *Oral Surg Oral Med Oral Pathol Oral Radiol.* 2017;123:468-476.
24. Lewis JS, Beadle B, Bishop JA, et al. Human papillomavirus testing in head and neck carcinomas: guideline from the College of American Pathologists. *Arch Pathol Lab Med.* 2018;142:559-597.
25. Yamamoto H, Kohashi K, Fujita A, Oda Y. Fascin-1 overexpression and miR-133b downregulation in the progression of gastrointestinal stromal tumor. *Mod Pathol.* 2013;26:563-571.
26. Ellrott K, Bailey MH, Saksena G, et al. Scalable open science approach for mutation calling of tumor exomes using multiple genomic pipelines. *Cell Syst.* 2018;6:271-281.e7.
27. Köbel M, Piskorz AM, Lee S, et al. Optimized p53 immunohistochemistry is an accurate predictor of TP53 mutation in ovarian carcinoma. *J Pathol Clin Res.* 2016;2:247-258.
28. Murnyák B, Hortobágyi T. Immunohistochemical correlates of TP53 somatic mutations in cancer. *Oncotarget.* 2016;7:64910-64920.
29. Campbell JD, Yau C, Bowlby R, et al. Genomic, pathway network, and immunologic features distinguishing squamous carcinomas. *Cell Rep.* 2018;23:194-212.e6.
30. Dzikiewicz-Krawczyk A, Kok K, Slezak-Prochazka I, et al. ZDHHC11 and ZDHHC11B are critical novel components of the oncogenic MYC-miR-150-MYB network in Burkitt lymphoma. *Leukemia.* 2017;31:1470-1473.
31. Hedberg ML, Goh G, Chiosea SI, et al. Genetic landscape of metastatic and recurrent head and neck squamous cell carcinoma. *J Clin Invest.* 2016;126:169-180.
32. Gao Y-B, Chen Z-L, Li J-G, et al. Genetic landscape of esophageal squamous cell carcinoma. *Nat Genet.* 2014;46:1097-1102.
33. Li YY, Hanna GJ, Laga AC, Haddad RI, Lorch JH, Hammerman PS. Genomic analysis of metastatic cutaneous squamous cell carcinoma. *Clin Cancer Res.* 2015;21:1447-1456.
34. Fehringer G, Kraft P, Pharoah PD, et al. Cross-cancer genome-wide analysis of lung, ovary, breast, prostate, and colorectal cancer reveals novel pleiotropic associations. *Cancer Res.* 2016;76:5103-5114.
35. Tanikawa C, Kamatani Y, Toyoshima O, et al. Genome-wide association study identifies gastric cancer susceptibility loci at 12q24.11-12 and 20q11.21. *Cancer Sci.* 2018;109:4015-4024.
36. Pytynia KB, Dahlstrom KR, Sturgis EM. Epidemiology of HPV-associated oropharyngeal cancer. *Oral Oncol.* 2014;50:380-386.
37. Tsunoda A, Sumi T, Terasaki O, Kishimoto S. Right dominance in the incidence of external auditory canal squamous cell carcinoma in the Japanese population: Does handedness affect carcinogenesis? *Laryngoscope Investig Otolaryngol.* 2017;2:19-22.
38. Yin M, Ishikawa K, Honda K, et al. Analysis of 95 cases of squamous cell carcinoma of the external and middle ear. *Auris Nasus Larynx.* 2006;33:251-257.
39. Cho RJ, Alexandrov LB, den Breems NY, et al. APOBEC mutation drives early-onset squamous cell carcinomas in recessive dystrophic epidermolysis bullosa. *Sci Transl Med.* 2018;10:eaas9668.
40. Masterson L, Winder DM, Marker A, et al. Investigating the role of human papillomavirus in squamous cell carcinoma of the temporal bone. *Head Neck Oncol.* 2013;5:1-8.
41. Saladi SV, Ross K, Karaayvaz M, et al. ACTL6A is co-amplified with p63 in squamous cell carcinoma to drive yap activation, regenerative proliferation, and poor prognosis. *Cancer Cell.* 2017;31:35-49.
42. Zack TI, Schumacher SE, Carter SL, et al. Pan-cancer patterns of somatic copy number alteration. *Nat Genet.* 2013;45:1134-1140.
43. Priestley P, Baber J, Lolkema MP, et al. Pan-cancer whole-genome analyses of metastatic solid tumours. *Nature.* 2019;575:210-216.
44. Wolfgang CD, Lee B, Pastan I, Essand M. T-cell receptor  $\gamma$  chain alternate reading frame protein (TARP) expression in prostate cancer cells leads to an increased growth rate and induction of caveolins and amphiregulin. *Cancer Res.* 2001;61:8122-8126.
45. Wolfgang CD, Essand M, Vincent JJ, Lee B, Pastan I. TARP: A nuclear protein expressed in prostate and breast cancer cells derived from an alternate reading frame of the T cell receptor  $\gamma$  chain locus. *Proc Natl Acad Sci USA.* 2000;97:9437-9442.
46. Huang L, Liu Q, Lang G-T, Cao A-Y, Shao Z-M. Concordance of hormone receptor status and BRCA1/2 mutation among women with synchronous bilateral breast cancer. *Front Oncol.* 2020;10:1-7.
47. Yin X, Jing Y, Cai M-C, et al. Clonality, heterogeneity, and evolution of synchronous bilateral ovarian cancer. *Cancer Res.* 2017;77:6551-6561.
48. Davoli T, Xu A, Mengwasser K, et al. Cumulative haploinsufficiency and triplosensitivity drive aneuploidy patterns and shape the cancer genome. *Cell.* 2013;155:948-962.
49. Sato K, Masuda T, Hu Q, et al. Novel oncogene 5MP1 reprograms c-Myc translation initiation to drive malignant phenotypes in colorectal cancer. *EBioMedicine.* 2019;44:387-402.
50. Kouyama Y, Masuda T, Fujii A, et al. Oncogenic splicing abnormalities induced by DEAD-Box Helicase 56 amplification in colorectal cancer. *Cancer Sci.* 2019;110:3132-3144.
51. Bradner JE, Hnisz D, Young RA. Transcriptional addiction in cancer. *Cell.* 2017;168:629-643.
52. Yuan J, Jiang Y-Y, Mayakonda A, et al. Super-enhancers promote transcriptional dysregulation in nasopharyngeal carcinoma. *Cancer Res.* 2017;77:6614-6626.
53. Gimple RC, Kidwell RL, Kim LJY, et al. Glioma stem cell-specific superenhancer promotes polyunsaturated fatty-acid synthesis to support EGFR signaling. *Cancer Discov.* 2019;9:1248-1267.
54. Miyazaki M, Aoki M, Okado Y, et al. Poorly differentiated clusters predict a poor prognosis for external auditory canal carcinoma. *Head Neck Pathol.* 2018;1-10.

55. Okado Y, Aoki M, Hamasaki M, et al. Tumor budding and laminin5- $\gamma$ 2 in squamous cell carcinoma of the external auditory canal are associated with shorter survival. *Springerplus*. 2015;4:814.

#### SUPPORTING INFORMATION

Additional supporting information may be found online in the Supporting Information section.

**How to cite this article:** Sato K, Komune N, Hongo T, et al. Genetic landscape of external auditory canal squamous cell carcinoma. *Cancer Sci*. 2020;111:3010–3019. <https://doi.org/10.1111/cas.14515>